Pergamon

PII: S0042-6989(97)00104-1

Vision Res., Vol. 37, No. 17, pp. 2325–2330, 1997

Printed in Great Britain
0042-6989/97 $17.00 + 0.00

Rapid Communication

Concentric Orientation Summation in Human Form Vision

HUGH R. WILSON,*‡ FRANCES WILKINSON,† WAEL ASAAD*

Received 17 December 1996; in revised form 1 April 1997

Psychophysical data demonstrate that orientation information in concentric, random-dot Glass patterns is summed linearly to extract a global form percept. Surprisingly, no such global pooling was found for Glass patterns with parallel structure. A simple neural model explains these results and agrees with recent V4 single unit physiology. As V4 provides the major input to IT, global concentric units may play an important role in analyzing complex images such as faces. In support of this possibility, deficits in the perception of concentric Glass patterns have recently been linked to prosopagnosia. © 1997 Elsevier Science Ltd.

Form vision Spatial pooling V4 Glass pattern Random dots

INTRODUCTION

Neurons in primary visual cortex (V1) are selectively sensitive to the orientation of lines and edges (Hubel & Wiesel, 1962, 1968), while neurons at the highest levels of form vision in inferior temporal cortex (IT) respond selectively to global patterns such as faces (Gross, 1992; Desimone, 1991; Perrett & Chitty, 1987). This raises the question: how is V1 contour information converted into a form suitable for global pattern responses in IT? We have explored this issue in human vision by measuring thresholds for Glass (Glass, 1969; Glass & Pérez, 1973) pattern detection. Results show that all subjects are more sensitive to concentric structure than to hyperbolic, radial, or parallel structure in Glass patterns. Further experiments provide evidence for units which sum orientation information globally along concentric contours. A simple quantitative model for global pooling of orientation-selective V1 responses accounts for the human data and is also consistent with recent V4 physiology (Gallant *et al.*, 1993).

METHODS

Glass patterns (Glass, 1969; Glass & Pérez, 1973) are random dot patterns in which pairs of dots are positioned such that the orientation of each dot pair is tangent to contours of a global pattern. To construct the concentric Glass pattern in Fig. 1(A), dot pairs were positioned at random in the pattern, but the pair orientation was always tangent to a circle centered on the pattern. Radial and hyperbolic (i.e., where contours are described by xy = constant) Glass patterns, illustrated in Fig. 1(B and C), are constructed in a similar manner. Thresholds for detecting global structure in Glass patterns were measured by replacing a fraction of the oriented dot pairs by an equal number of randomly positioned "noise" dots. Preliminary experiments showed that thresholds did not vary over the dot density range from 3 to 12%, or for dot pair separations from 4.5 to 13.0 arc min. Accordingly, experiments were conducted with 10.0 arc min separation and a dot density of 6%. Under these conditions the mean dot spacing was 4.4 arc min, less than half the spacing between correlated dots in each pair. Individual dots were squares with 1.1 arc min sides, and all dots were white (except in the rectification experiments described later) on a gray background with mean luminance 63 cd/m^2.

Subjects viewed a Macintosh monitor that subtended 9 deg×12 deg and had a frame rate of 67 Hz. Each stimulus was 4.9 deg in diameter and centered on the monitor. (Control experiments in which the stimuli filled a 4.9 deg square produced the same results.) Stimuli were presented in a two temporal-interval forced-choice paradigm with one interval containing a percentage of signal dots defining a global structure and the other interval containing the same density of dots randomly positioned. Each pattern was presented for 167 msec to minimize the effects of eye movements. In a given experiment, patterns with four different signal percentages were used, and the percentage of signal dots at threshold (75% correct) was estimated by fitting a Quick (1974) or Weibull (1951) distribution using a maximum likelihood procedure.

*Visual Sciences Center, University of Chicago, 939 East 57th Street, Chicago, IL 60637, U.S.A.
†Department of Psychology, McGill University, 1205 Dr. Penfield Avenue, Montreal, QC H3A 1B1, Canada.
‡To whom all correspondence should be addressed [*Fax*: +1-773-702-4442; *Email*: hrw6@midway.uchicago.edu].

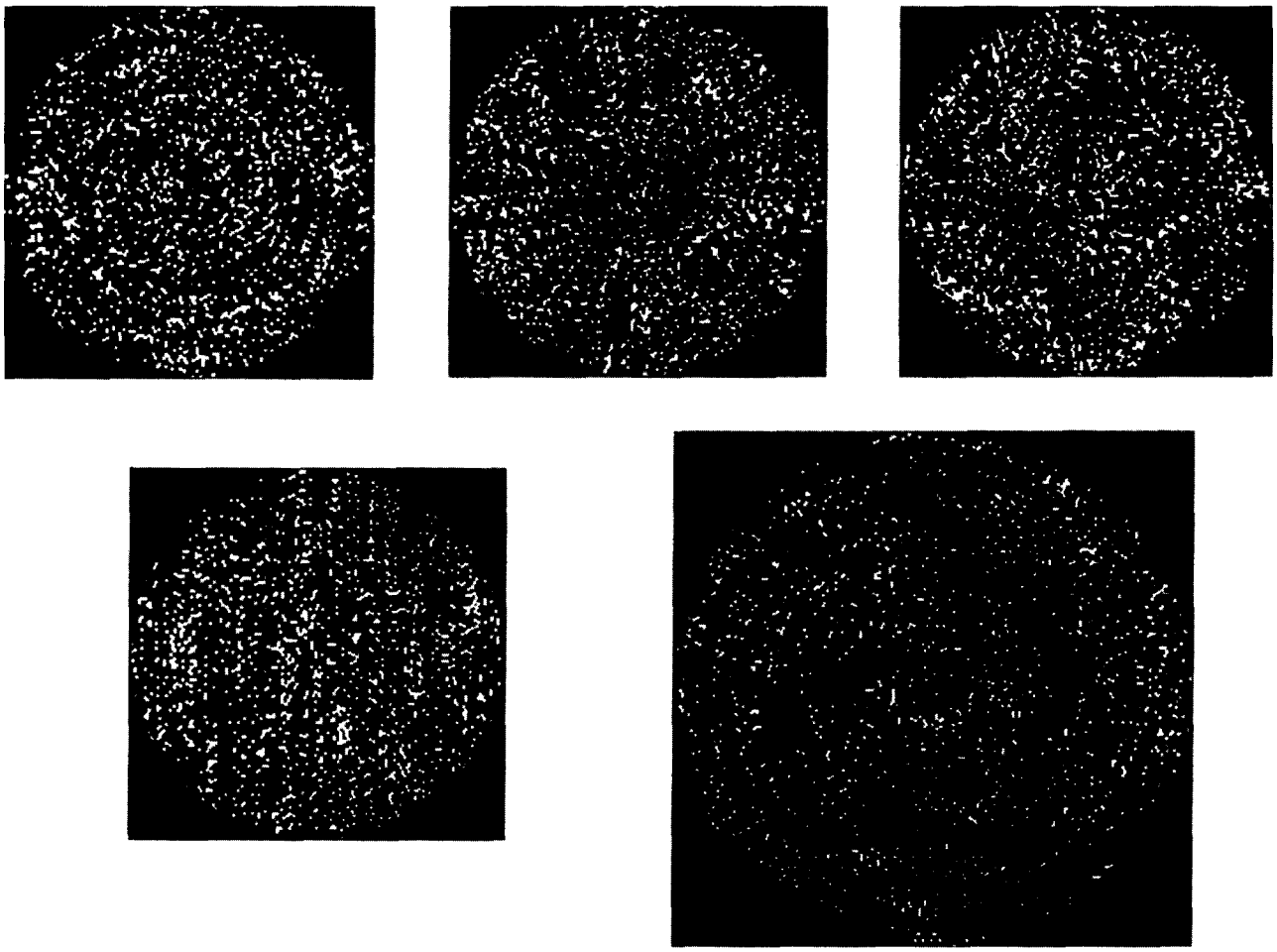

FIGURE 1. Glass patterns used in this study. Concentric, radial, hyperbolic, and parallel Glass patterns with 6% dot density and 10 arc min separation between paired signal dots are depicted in (A–D), respectively. The parallel Glass pattern in (D) contains two superimposed dashed lines (not present in the actual stimulus) to indicate the location of the vertical strip in area summation experiments. (An analogous horizontal strip was also used.) (E) illustrates a concentric Glass pattern containing 50% white dots and 50% black dots (the total dot density remaining at 6%). In this pattern, all of the white dots are paired signal dots, while all of the black dots constitute random noise. Subjects could not discriminate (E) from the reverse pattern in which the paired signal dots were all black, while the white dots constituted noise.

RESULTS

We first measured thresholds for Glass patterns containing concentric, radial, hyperbolic, and parallel structure. In each experiment the subject was informed which type of pattern would be presented. Results plotted on logarithmic coordinates in Fig. 2 demonstrate that all subjects had the lowest thresholds for concentric Glass patterns. All subjects also had the highest thresholds for parallel patterns with the dot pairs oriented vertically, while thresholds for radial and hyperbolic patterns were intermediate. Signal thresholds averaged across subjects were: concentric, 11.6%; radial, 24.1%; hyperbolic, 28.7%; parallel, 56.5%.

Given the very low thresholds for detecting concentric Glass patterns, these were selected for further study. To determine how the visual system extracts a global concentric percept, the patterns were notionally divided into 12 pie-wedge segments, and all signal dot pairs were restricted to a subset of these. As shown at the top of Fig. 3(A), a 50% signal area was constructed by restricting all signal dot pairs to alternate pie-wedges, while the intervening segments contained only noise dots. Thus, signal percentage for these patterns reflects the percentage of signal dot pairs within the signal areas. The mean density of dots in all segments remained constant. The graph in Fig. 3(A) shows that as the fraction of pattern area containing signal dots was reduced, the percentage of signal dots within those areas had to be increased substantially to reach threshold. Power functions were fit to the data, and the mean exponent was found to be -0.91, which did not differ significantly ($P > 0.20$ for every subject) from a value of -1.0. This indicates almost perfect summation of dot pair orientations concentrically around the pattern. That is, as signal dot pairs are replaced by noise in some of the pie-wedges, a similar of dot pairs must be added to the signal wedges to reach threshold.

To determine whether this concentric signal summation reflected global pattern properties rather than local dot statistics, we conducted a control experiment using parallel Glass patterns. All signal dot pairs in these

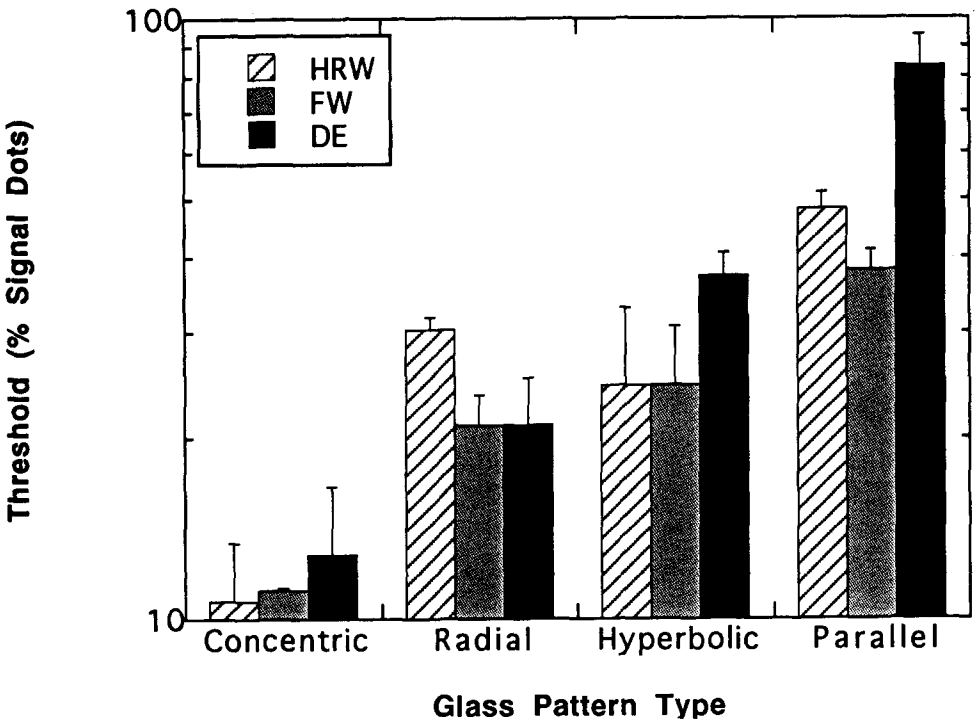

FIGURE 2. Threshold signal percentages for detecting global structure in Glass patterns. All subjects had 3.5–5.0 times lower thresholds for concentric than for parallel Glass patterns, while radial and hyperbolic thresholds were intermediate. Error bars in this and the next figure plot standard errors of the mean.

patterns were vertically oriented, and the signal dots were either present throughout the pattern, or else were restricted to a vertical [see Fig. 1(D)] or horizontal strip of constant width running through the center of the pattern. Although Fig. 2 shows that thresholds were highest for parallel Glass patterns, restricting the signal dots to 31% of the total area did not increase the threshold for any subject, as shown by mean data plotted by line P–P in Fig. 3(A). The ellipses encircling the Ps delimit the range of the data in each condition (36–49% for 100% signal area, and 41–46% for 31% signal area). Thus, there is no evidence for global summation in the detection of these parallel patterns. As concentric and parallel Glass patterns have highly similar *local* statistics, it may be concluded that linear summation in the former but not the latter reflects a *global* orientation pooling process optimized for concentric patterns.

A second summation experiment measured the radial extent of summation for concentric Glass patterns. Signal and noise areas were notionally separated at a critical radius, which produced two classes of patterns: those in which the signal was restricted to a center circle, and those in which the signal formed a surrounding annulus. Data in Fig. 3(B) show that the circle and annulus data cross at a radius of about 1.6 deg, indicating that signal summation extends out to about this radius.

Glass and Switkes (1976) had shown that if the two dots in each signal pair were of opposite contrasts (i.e., black and white), concentric structure was no longer visible. This was taken as presumptive evidence that the first stage of Glass pattern perception involves stimulation of V1 neurons that extract the orientation of individual signal dot pairs. However, full-wave rectification *following* oriented filtering has been reported in both texture (Bergen & Landy, 1991; Graham, 1991; Malik & Perona, 1990; Wilson & Richards, 1992) and second-order ("non-Fourier") motion perception (Chubb & Sperling, 1988, 1989; Wilson *et al.*, 1992). To determine whether full-wave rectification might also be involved in Glass pattern perception, therefore, we devised novel patterns containing 50% black dots and 50% white dots. A glance at Fig. 1(E) will confirm that these patterns contain a clearly visible concentric Glass signal. What is not evident without scrutiny is that all of the white dots in Fig. 1(E) are signal dot pairs, while the black dots are entirely random. Subjects were asked to discriminate patterns like Fig. 1(E) from ones in which all signal dots were black and all noise dots were white in a two-interval forced-choice experiment. None of seven subjects could discriminate these two pattern types above chance, the mean performance being 54% correct. In control experiments, subjects were all greater than 95% correct at detecting the global concentric structure in these patterns; they simply could not discriminate which dots conveyed the concentric structure. This provides strong evidence for full-wave rectification *following* oriented filtering.

MODEL

These Glass pattern thresholds can be explained quantitatively by the simple model depicted in Fig. 4. This model first applies oriented filtering to the image at six different orientations separated by 30 deg each (only three are illustrated). Filter characteristics have been

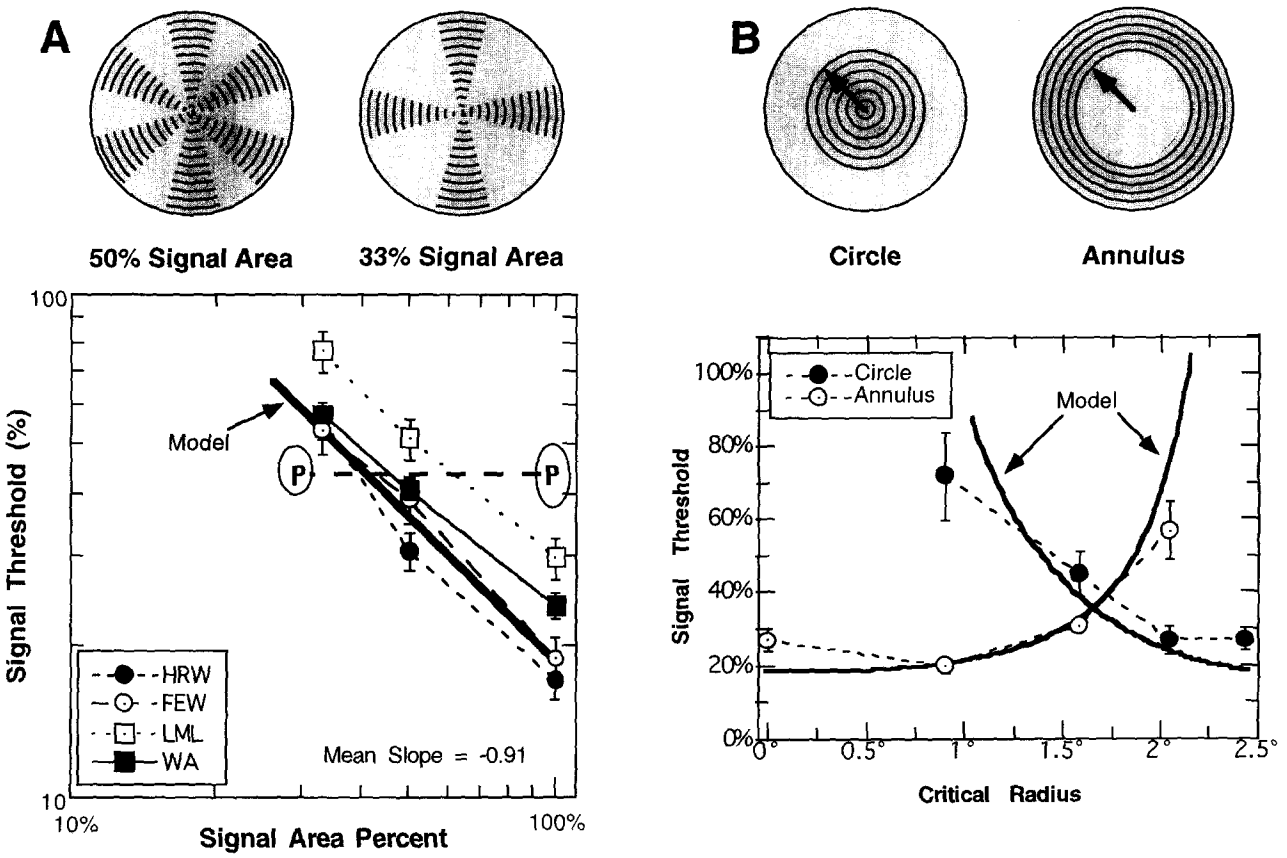

FIGURE 3. Area summation results for concentric Glass patterns. The data in (A) were obtained by notionally dividing the pattern into 12 pie-wedges and restricting the signal dots to a fraction of the wedges. This is shown schematically above the graph for 50 and 33% signal areas, where gray represents noise dots and concentric arcs indicate regions that contained signal dots. All four subjects showed a reciprocal linear relationship in log–log coordinates between signal area and Glass pattern threshold. Power functions fit to the data showed a mean slope of −0.91. Thresholds were also obtained using parallel Glass patterns in which the signal dots were restricted to either a vertical [see Fig. 1(D)] or a horizontal strip through the pattern center, and line P–P shows mean data for four subjects. The range of the results across subjects is encompassed by the two ovals. The lack of any areal summation in this case shows that it is the global rather than local structure of concentric patterns that is responsible for concentric summation. (B) depicts an analogous experiment in which dots were restricted either to a centered circle or to a surrounding annulus (critical radii shown by arrows at top). Data curves show the mean and range for two subjects. Heavy curves marked "Model" in the two graphs plot Monte-Carlo predictions of the neural model depicted in Fig. 4.

previously estimated by masking (Wilson *et al.*, 1983; Wilson, 1991) and are in good agreement with single unit data from primate V1 (DeValois *et al.*, 1982). Each filtered image is then full-wave rectified and filtered again by a pair of oriented, center–surround filters. Following initial horizontal filtering, for example, the second stage filters are vertically oriented and positioned at equal distances above and below the model receptive field center (second pathway in Fig. 4). The equation for this pair of filters is:

$$W(x,y) = \left\{3\exp\left(\frac{-x^2}{0.5^2}\right) - \exp\left(\frac{-x^2}{1.5^2}\right)\right\}\exp\left(\frac{-(y-y_0)^2}{0.8^2}\right) + \left\{3\exp\left(\frac{-x^2}{0.5^2}\right) - \exp\left(\frac{-x^2}{1.5^2}\right)\right\}\exp\left(\frac{-(y+y_0)^2}{0.8^2}\right) \quad (1)$$

where $y_0 = 1.4$ deg, and all parameters were chosen based on the data in Fig. 3(B). This combination of filtering, rectification, and subsequent orthogonal filtering simply produces a pair of complex, end-stopped model cells (Wilson, 1997). Previous work has shown that such end-stopped cells can encode contour curvature (Dobbins *et al.*, 1987; Koenderink & Richards, 1988; Wilson & Richards, 1992). Other pathways are simply rotated versions of this one, so the relationship between first- and second-stage filters results in summation of curvature information that is roughly concentric with the filter center. Finally, these parallel filter–rectify–filter pathways are summed and passed through a threshold function.

This model was implemented in MatLab as a Monte-Carlo simulation. Briefly, large numbers of Glass patterns were processed by the model in order to estimate the mean and standard deviation of the response as a function of signal dot percentage. From these results it was possible to estimate the signal percentage necessary for 75% correct discrimination by the model. Model predictions for detection of concentric Glass patterns

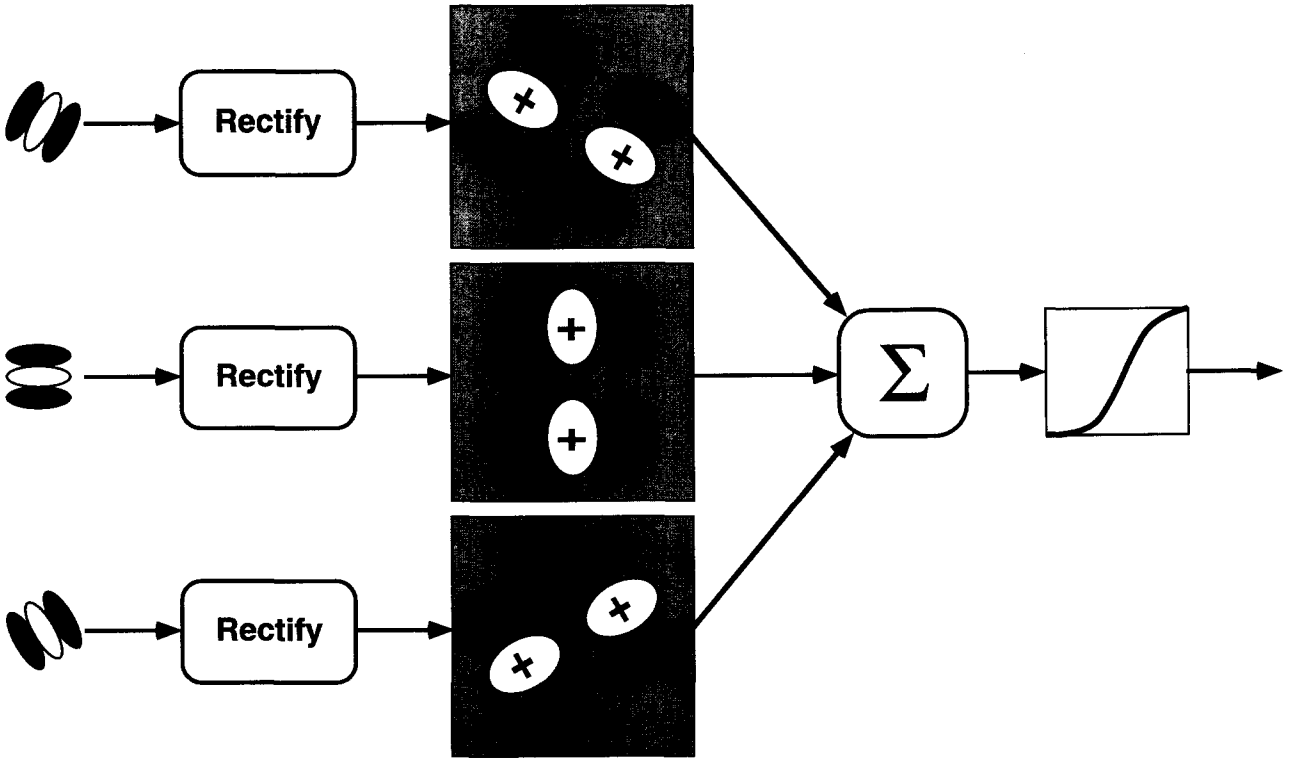

FIGURE 4. Schematic of a neural model consistent with Glass pattern data and with responses of non-Cartesian units in V4 (Gallant *et al.*, 1993, 1996). The model contains six parallel pathways (only three shown), each involving oriented filtering followed by full-wave rectification and second-stage filtering. Second-stage filters are pairs of excitatory center (+), inhibitory surround units oriented at right angles to the first-stage filters. This results in an array of concentrically organized, end-stopped units that are sensitive to contour curvature (Dobbins *et al.*, 1987; Koenderink & Richards, 1988; Wilson & Richards, 1992). As there is summation over a range of radii, the model responds to quasi-circular stimuli over a considerable size range. Summation of all six pathways followed by a threshold response function completed the model.

are plotted in Fig. 3, where consistency with the data is good.

DISCUSSION

Thresholds for detecting Glass (1969) patterns in noise provide clear evidence for global summation of concentrically arranged orientations in human vision. Surprisingly, however, there is no evidence for global pooling in the detection of parallel Glass patterns, thus suggesting that parallel structure is only processed locally. In a study analogous to ours Morrone *et al.* (1995) used moving random dot patterns and discovered evidence for units tuned to circular motion. Following local orientation and motion extraction in V1, therefore, the visual system may employ similar computational strategies to extract global patterns of both form and motion.

The nonlinear model that accounts for Glass pattern thresholds is also consistent with physiology of the primate form vision pathway. The filter–rectify–filter sequences in Fig. 4 are just second-order or "non-Fourier" pathways used to explain both texture boundary extraction (Bergen & Landy, 1991; Graham, 1991; Malik & Perona, 1990; Wilson & Richards, 1992) and the responses of V2 neurons to illusory contours (von der Heydt *et al.*, 1984, 1989) and curvature (Dobbins *et al.*, 1987; Koenderink & Richards, 1988). In agreement with V4 physiology (Gallant *et al.*, 1993, 1996), simulations showed that the final model stage responded much more strongly to concentric cosines than to either hyperbolic or conventional cosine gratings, and the model was insensitive to the exact positioning of the stimulus. In further accord with V4 physiology, the model receptive field was much larger than the first stage filters, but the spatial frequency tuning was similar to that of V1 neurons (Desimone & Schein, 1987).

Although we have presented a "hard-wired" model, similar models could doubtless be produced through Hebbian learning in a manner analogous to that proposed for optic flow units in area MST (Zhang *et al.*, 1993). However, any such learning probably occurs early in life, as studies have shown that very young kittens discriminate concentric from radial patterns more effectively than horizontal from vertical gratings (Wilkinson & Dodwell, 1980; Dodwell *et al.*, 1983).

Image processing simulations show that our model concentric units respond strongly to the quasi-circular contours delimiting human faces over a range of head sizes and orientations (Wilson, 1997). Furthermore, damage to primate area V4 leads to severe deficits in form vision (Heywood *et al.*, 1992; Merigan, 1996). Finally, it has been reported that a prosopagnosic patient also showed selective deficits in perceiving concentric Glass patterns (Rentschler *et al.*, 1994). Thus, we

conjecture that V4 concentric units form a key link between local V1 orientation processing and global face perception in IT.

REFERENCES

Bergen, J. R. & Landy, M. S. (1991). Computational modeling of visual texture segregation. In Landy, M. & Movshon, J. A. (Eds), *Computational Models of Visual Processing* (pp. 253–271). Cambridge, MA: MIT Press.

Chubb, C. & Sperling, G. (1988). Drift-balanced random stimuli: a general basis for studying non-Fourier motion perception. *Journal of the Optical Society of America A, 5*, 1986–2007.

Chubb, C. & Sperling, G. (1989). Two motion perception mechanisms revealed through distance-driven reversal of apparent motion. *Proceedings of the National Academy of Sciences USA, 86*, 2985–2989.

Desimone, R. (1991). Face selective cells in the temporal cortex of monkeys. *Journal of Cognitive Neuroscience, 3*, 1–8.

Desimone, R. & Schein, S. J. (1987). Visual properties of neurons in area V4 of the macaque: sensitivity to stimulus form. *Journal of Neurophysiology, 57*, 835.

DeValois, R. L., Albrecht, D. G. & Thorell, L. G. (1982). Spatial frequency selectivity of cells in macaque visual cortex. *Vision Research, 22*, 545–559.

Dobbins, A., Zucker, S. W. & Cynader, M. S. (1987). Endstopped neurons in the visual cortex as a substrate for calculating curvature. *Nature, 329*, 438–441.

Dodwell, P. C., Wilkinson, F. E. & von Grünau, M. W. (1983). Pattern recognition in kittens: performance on Lie patterns. *Perception, 12*, 393–410.

Gallant, J. L., Braun, J. & VanEssen, D. C. (1993). Selectivity for polar, hyperbolic, and Cartesian gratings in macaque visual cortex. *Science, 259*, 100–103.

Gallant, J. L., Connor, C. E., Rakshit, S., Lewis, J. W. & Van Essen, D. C. (1996). Neural responses to polar, hyperbolic, and Cartesian gratings in area V4 of the macaque monkey. *Journal of Neurophysiology, 76*, 2718–2739.

Glass, L. (1969). Moiré effect from random dots. *Nature, 223*, 578–580.

Glass, L. & Pérez, R. (1973). Perception of random dot interference patterns. *Nature, 246*, 360–362.

Glass, L. & Switkes, E. (1976). Pattern recognition in humans: correlations which cannot be perceived. *Perception, 5*, 67–72.

Graham, N. (1991) Complex channels, early local nonlinearities, and normalization in texture segregation. In Landy, M. & Movshon, J. A. (Eds), *Computational models of visual processing*. Cambridge, MA: MIT Press.

Gross, C. G. (1992). Representation of visual stimuli in inferior temporal cortex. *Philosophical Transactions of the Royal Society of London B, 335*, 3–10.

Heywood, C. A., Gadotti, A. & Cowey, A. (1992). Cortical area V4 and its role in the perception of color. *Journal of Neuroscience, 12*, 4056–4065.

Hubel, D. H. & Wiesel, T. N. (1962). Receptive fields, binocular interaction, and functional architecture in the cat's striate cortex. *Journal of Physiology, 160*, 106–154.

Hubel, D. H. & Wiesel, T. N. (1968). Receptive fields and functional architecture of monkey striate cortex. *Journal of Physiology, 195*, 215–243.

Koenderink, J. J. & Richards, W. (1988). Two-dimensional curvature operators. *Journal of the Optical Society of America A, 5*, 1136–1141.

Malik, J. & Perona, P. (1990). Preattentive texture discrimination with early vision mechanisms. *Journal of the Optical Society of America A, 7*, 923–932.

Merigan, W. H. (1996). Basic visual capabilities and shape discrimination after lesions of extrastriate area V4 in macaques. *Visual Neuroscience, 13*, 51–60.

Morrone, M. C., Burr, D. C. & Vaina, L. M. (1995). Two stages of visual processing for radial and circular motion. *Nature, 376*, 507–509.

Perrett, D. I. & Chitty, A. J. (1987). Visual neurones responsive to faces. *Trends in Neuroscience, 10*, 358–364.

Quick, R. F. (1974). A vector-magnitude model of contrast detection. *Kybernetik, 16*, 1299–1302.

Rentschler, I., Treutwein, B. & Landis, T. (1994). Dissociation of local and global processing in visual agnosia. *Vision Research, 34*, 963–971.

von der Heydt, R. & Peterhans, E. (1990). Mechanisms of contour perception in monkey visual cortex. I. Lines of pattern discontinuity. *Journal of Neuroscience, 9*, 1731–1748.

von der Heydt, R., Peterhans, E. & Baumgartner, G. (1984). Illusory contours and cortical neuron responses. *Science, 224*, 1260–1262.

Weibull, W. A. (1951). A statistical distribution function of wide applicability. *Journal of Applied Mechanics, 18*, 292–297.

Wilkinson, F. & Dodwell, P. C. (1980). Young kittens can learn complex visual pattern discriminations. *Nature, 284*, 258–259.

Wilson, H. R., McFarlane, D. K. & Phillips, G. C. (1983). Spatial frequency tuning of orientation selective units estimated by oblique masking. *Vision Research, 23*, 873–882.

Wilson, H. R. (1991). Psychophysical models of spatial vision and hyperacuity. In Regan, D. (Ed.), *Spatial vision* (pp. 64–86). London: MacMillan.

Wilson, H. R. (1997). Non-Fourier cortical processes in texture, form, and motion perception. In Ulinski, P. S. & Jones, E. G. (Eds), *Cerebral cortex, models of cortical circuitry* (Vol. 14). New York: Plenum.

Wilson, H. R., Ferrera, V. P. & Yo, C. (1992). Psychophysically motivated model for two-dimensional motion perception. *Visual Neuroscience, 9*, 79–97.

Wilson, H. R. & Richards, W. A. (1992). Curvature and separation discrimination at texture boundaries. *Journal of the Optical Society of America A, 9*, 1653–1662.

Zhang, K., Sereno, M. I. & Sereno, M. E. (1993). Emergence of position-independent detectors of sense of rotation and dilation with Hebbian learning: an analysis. *Neural Computation, 5*, 597–612.

Acknowledgements—HRW was supported in part by NIH grant No. EY02158 and by grants from Research to Prevent Blindness and the Brain Research Foundation to The University of Chicago. FW was supported in part by NCERC No. OGP0007551 (Canada).